

Rho-kinase inhibition has antidepressant-like efficacy and expedites dendritic spine pruning in adolescent mice

Lauren P. Shapiro^{a,b,c}, Henry W. Kietzman^{b,c,d}, Jidong Guo^{c,e}, Donald G. Rainnie^{c,e}, Shannon L. Gourley^{a,b,c,d,e,*}

^a Molecular and Systems Pharmacology, Emory University, Atlanta, GA, United States

^b Department of Pediatrics, Emory University School of Medicine, Atlanta, GA, United States

^c Yerkes National Primate Research Center, Emory University, Atlanta, GA, United States

^d Graduate Program in Neuroscience, Emory University, Atlanta, GA, United States

^e Department of Psychiatry, Emory University School of Medicine, Atlanta, GA, United States

ARTICLE INFO

Keywords:

Forced swim

Novelty suppressed feeding

Protein kinase B

HA-1077

ROCKII

Slx-2119

Rho-associated coiled-coil containing kinase

ABSTRACT

Adolescence represents a critical period of neurodevelopment, defined by structural and synaptic pruning within the prefrontal cortex. While characteristic of typical development, this structural instability may open a window of vulnerability to developing neuropsychiatric disorders, including depression. Thus, therapeutic interventions that support or expedite neural remodeling in adolescence may be advantageous. Here, we inhibited the neuronally-expressed cytoskeletal regulatory factor Rho-kinase (ROCK), focusing primarily on the clinically-viable ROCK inhibitor fasudil. ROCK inhibition had rapid antidepressant-like effects in adolescent mice, and its efficacy was comparable to ketamine and fluoxetine. It also modified levels of the antidepressant-related signaling factors, tropomyosin/tyrosine receptor kinase B and Akt, as well as the postsynaptic marker PSD-95, in the ventromedial prefrontal cortex (vmPFC). Meanwhile, adolescent-typical dendritic spine pruning on excitatory pyramidal neurons in the vmPFC was expedited. Further, vmPFC-specific shRNA-mediated reduction of ROCK2, the dominant ROCK isoform in the brain, had antidepressant-like consequences. We cautiously suggest that ROCK inhibitors may have therapeutic potential for adolescent-onset depression.

1. Introduction

Depression is a major public health concern costing the United States \$99 billion in medical expenses annually (Greenberg et al., 2015). According to the 2015 National Survey on Drug Use and Health, 12.5% of youth ages 12–17 had a major depressive episode within the past year, and only 45% of these individuals received treatment (Substance Abuse and Mental Health Services Administration, 2017). In 2004, the FDA issued a black box warning regarding the use of antidepressants for individuals under the age of 25 due to a heightened risk of suicidal ideation. Although some more recent studies have scrutinized this policy, physicians remain reticent to prescribe antidepressants to adolescents (Isacson and Rich, 2014). As a result, there is a dire need for novel antidepressants suitable for adolescents and young adults.

During adolescence, the prefrontal cortex (PFC), a brain region that provides “top-down” control over emotion and behavior, undergoes dramatic structural reorganization and synaptic remodeling. Some

dendritic spines and synapses are refined, whereas others are pruned (Bourgeois et al., 1994; Huttenlocher and Dabholkar, 1997; Rakic et al., 1994; Shapiro et al., 2017). Although the molecular mechanisms mediating these events are not fully understood, some research suggests that structural instability may contribute to vulnerability to neuropsychiatric diseases (Keshavan et al., 2014). Thus, expediting or otherwise enhancing the structural remodeling that occurs during adolescence may be therapeutic in the treatment of adolescent-onset depression.

An important factor in regulating dendritic spine structure, including during adolescence, is the RhoA GTPase substrate Rho-kinase (ROCK) (Koleske, 2013; Maekawa et al., 1999; Murakoshi et al., 2011; Schubert et al., 2006). There are two isoforms of ROCK: ROCK1 and ROCK2, the latter more highly expressed in brain tissue (Duffy et al., 2009; Julian and Olson, 2014; Nakagawa et al., 1996). ROCK2 inhibits cofilin-mediated actin cycling, the process by which the equilibrium between monomeric, globular-actin (G-actin) and polymeric, filamentous-actin (F-actin) alters the size and shape of dendritic spines

* Corresponding author at: Yerkes National Primate Research Center, Emory University, 954 Gatewood Rd. NE, Atlanta, GA 30329, United States.

E-mail address: shannon.l.gourley@emory.edu (S.L. Gourley).

<https://doi.org/10.1016/j.nbd.2018.12.015>

Received 2 August 2018; Received in revised form 15 November 2018; Accepted 21 December 2018

Available online 26 December 2018

0969-9961/ © 2019 Elsevier Inc. All rights reserved.

(dos Remedios et al., 2003; Pontrello and Ethell, 2009). ROCK2 inhibits cofilin and can prevent changes in the morphology of the dendritic spine (Maekawa et al., 1999; Zhou et al., 2009). Pharmacological inhibition of ROCK2 can thus *promote* activity-dependent dendritic spine pruning or spine head enlargement (stabilization), depending on the extracellular milieu (Murakoshi et al., 2011; Schubert et al., 2006) and in other contexts, can enhance neurite outgrowth (discussed in (Harbom et al., 2018)). The ROCK inhibitor, fasudil, has a favorable pharmacological profile in humans: it is in clinical use, has oral bioavailability and minimal side effects, and readily crosses the blood brain barrier (Chen et al., 2013).

Here we report that the antidepressant-like potential of fasudil in adolescent mice is comparable to that of the commonly prescribed antidepressant fluoxetine (Prozac) and the novel antidepressant, subanaesthetic ketamine. We find that fasudil enhances the ratio of active/inactive TrkB and elevates Akt, signaling factors associated with antidepressant action. Fasudil also expedites dendritic spine pruning on excitatory neurons in the ventromedial prefrontal cortex (vmPFC). Further, shRNA-mediated silencing of the neuronal ROCK2 isoform selectively within the vmPFC also has antidepressant-like effects. Together, these findings suggest that inhibiting ROCK in the vmPFC enriches adolescent-typical dendritic spine pruning and has antidepressant-like potential. Importantly, systemic fasudil treatment was neither sedative, nor did it alter PFC-dependent learning and memory in adolescents, and it had virtually no antidepressant-like effects in adults. These findings identify ROCK inhibitors, including fasudil, as potential antidepressant agents well-suited to adolescent populations.

2. Results

The development of novel antidepressant agents suitable for adolescents is an urgent medical need. Here we characterize the effects of the ROCK inhibitor, fasudil, in tests of antidepressant-like efficacy designed for use in healthy rodents (as opposed to models of depression), and on PFC neurobiology in adolescent and adult mice.

2.1. ROCK inhibition has antidepressant-like potential in adolescent mice

To begin, we evaluated the antidepressant-like potential of fasudil in the forced swim test (FST), a rapid screen used to predict antidepressant efficacy, in adolescent male and female mice. Fasudil decreased time spent immobile, an antidepressant-like effect, in both

sexes [main effect of fasudil $F_{(1,42)} = 14.24, p = .012$, no interactions] (Fig. 1a). Fasudil did not impact locomotor activity at the time of test (Fig. S1a,b), and the antidepressant-like effect of fasudil was dose-dependent (Fig. S1c). Fasudil was administered 3 times over the course of 24 h, as a single injection did not have antidepressant-like consequences (Fig. S1d-f).

Next, we compared the effects of fasudil to those of fluoxetine and ketamine in adolescent female mice, given that depression is more prevalent in women. Ketamine's antidepressant-like efficacy in adolescent rodents is limited (Nosyreva et al., 2014), so it was not surprising when we observed highly variable responses to ketamine, despite utilizing a dose that has antidepressant-like effects in adult mice (Franceschelli et al., 2015). As a result, a median split was applied to identify ketamine “responders” and “non-responders” (Fig. S2a). In the FST, fasudil-treated mice were indistinguishable from ketamine “responders” and fluoxetine-treated mice, reducing immobility time compared to saline-treated mice [$F_{(3,45)} = 7.01, p = .001$] (Fig. 1b).

One limitation of the FST is that it lacks face validity, meaning, drugs like fluoxetine are efficacious 30 min after administration in the FST but may take ≥ 4 –6 weeks to affect clinical populations. We were thus interested in testing the efficacy of fasudil in a test that is predictive of therapeutic onset, so we used the novelty suppressed feeding (NSF) test (Ramaker and Dulawa, 2017). Here, fasudil-treated mice and ketamine “responders” generated lower latencies to approach a novel food than control mice, indicative of rapid antidepressant-like responses [$F_{(3,35)} = 4.71, p = .007$] (Fig. 1c, S2b). Fluoxetine did not impact NSF performance, expected given that chronic treatment is necessary for antidepressant action in humans.

Although ROCK2 is the dominant ROCK isoform in the central nervous system, ROCK1 is also present in the brain. Thus, we evaluated the effects of the novel ROCK2-specific inhibitor, SLX-2119. As with fasudil, SLX-2119 decreased the time spent immobile in the FST in adolescent female mice [$t_{(15)} = 1.90, p = .039$] (Fig. 1d). Notably, we identified a modest (though statistically non-significant) sedative effect of SLX-2119 (Fig. S3a,b); thus, even with blunted locomotor activity, SLX-2119 mice spent more time mobile than control mice, indicating that ROCK2 inhibition has antidepressant-like efficacy.

2.2. ROCK inhibition has differential neurobehavioral effects in adolescent and adult mice

Next, we evaluated the antidepressant-like potential of fasudil in

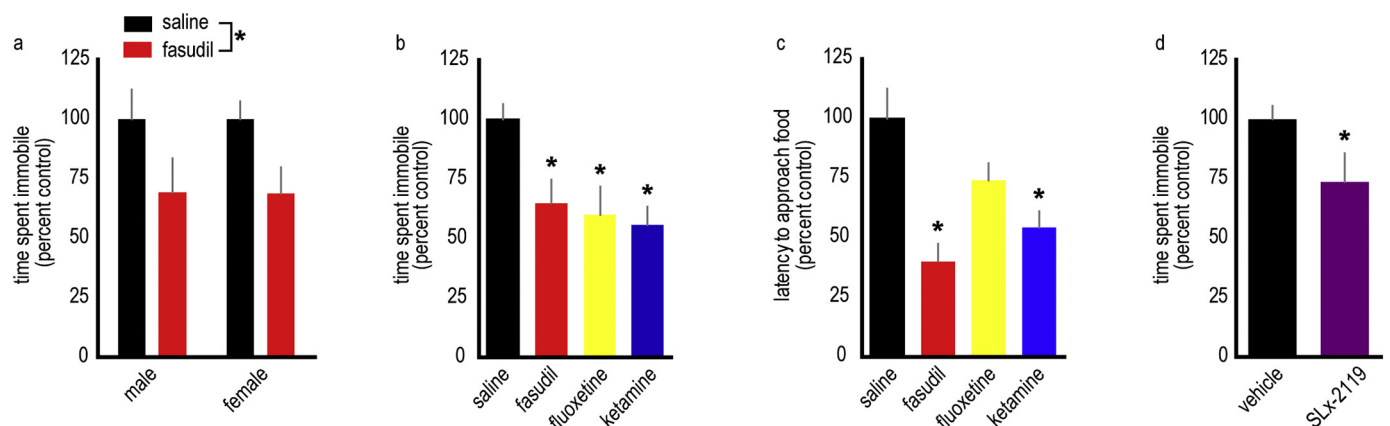


Fig. 1. ROCK inhibition has antidepressant-like efficacy in adolescent mice. **A.** The ROCK inhibitor fasudil has an antidepressant-like effects in adolescent male and female mice, indicated by a reduction in the time spent immobile in the forced swim test. $n = 11$ –12/group. **B.** The effects of fasudil are comparable to those of fluoxetine and ketamine in adolescent female mice. $n = 6$ –9/experimental group, with a combined control sample size of 26. **C.** Further, fasudil reduces latency to approach food in the novelty suppressed feeding task, suggesting that its effects may be rapid. $n = 8$ /group with a combined control sample size of 14. **D.** SLX-2119, a highly specific ROCK2 inhibitor, recapitulates the antidepressant-like effects of fasudil in the forced swim test, indicating that ROCK2 inhibition has antidepressant-like efficacy. $n = 8$ –9/group. All adolescent mice are P42, and all experiments were conducted exclusively in female mice with the exception Fig. 1a. Means + SEMs, * $p < .05$.

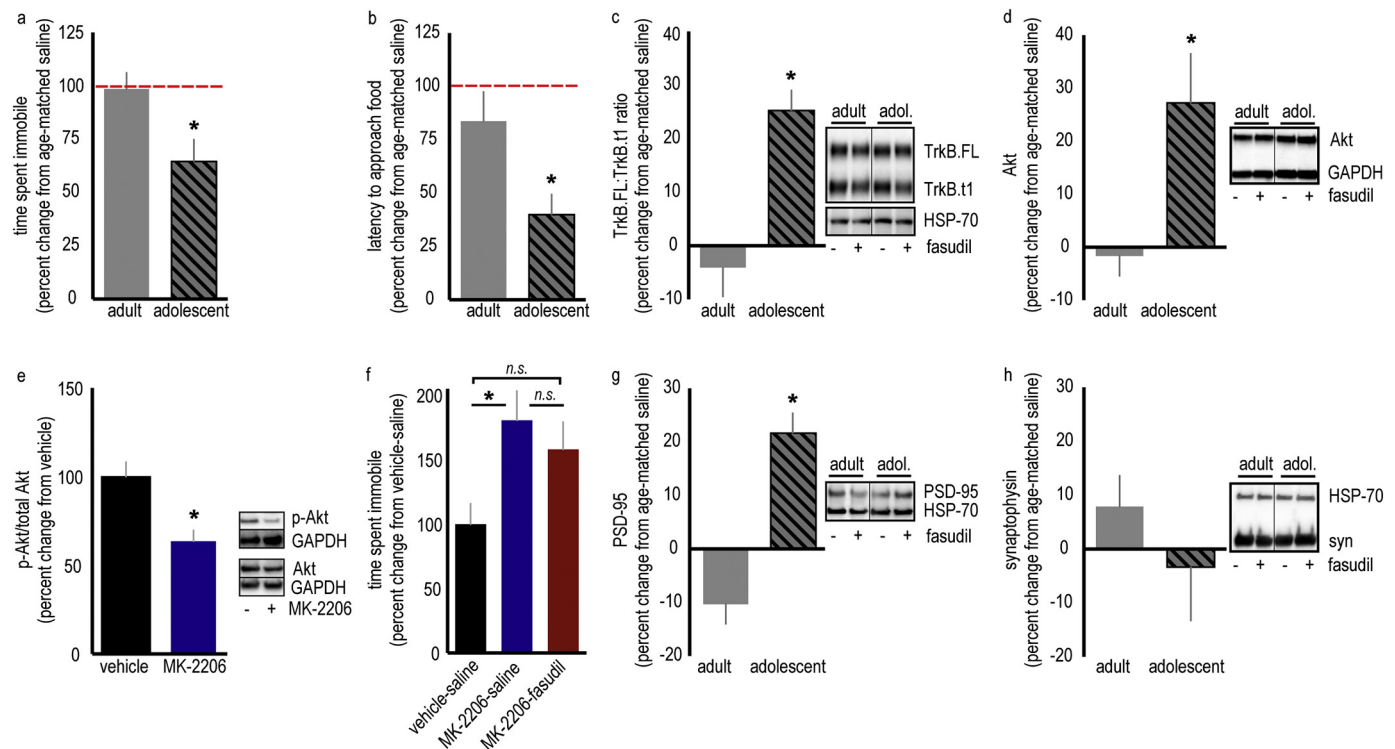


Fig. 2. ROCK inhibition has differential effects on adult and adolescent female mice, enriching TrkB.FL/TrkB.t1, Akt and PSD-95 in the adolescent vmPFC. A. Fasudil has antidepressant-like efficacy in adolescent mice, but not adult mice, in the forced swim test and (B) the novelty suppressed feeding test. The dashed line represents age-matched control mice. Raw immobility values are provided in Tables 1a and 1b. $n = 7-9$ /group (forced swim test) and $8-10$ /group (novelty suppressed feeding test). C. The TrkB receptor is implicated in the efficacy of several distinct antidepressants. Fasudil increases the ratio of the “active” TrkB.FL isoform relative to the “inactive” TrkB.t1 isoform in the vmPFC of adolescent, but not adult, mice. $n = 7$ /group. D. Fasudil also increases levels of the downstream signaling factor Akt in adolescent, but not adult, mice. $n = 8-10$ /group. E. The Akt inhibitor MK-2206 was administered systemically at a dose that decreases phosphorylated (p)-Akt levels in the vmPFC. $n = 4-7$ /group. F. Co-administration of MK-2206 and fasudil to adolescent mice occludes the antidepressant-like effects of fasudil in the forced swim test. $n = 6-7$ /group. G. Fasudil also elevates PSD-95 in the vmPFC. $n = 6-8$ /group. H. By contrast, fasudil does not alter the presynaptic marker, synaptophysin (syn). $n = 7-8$ /group. HSP-70 and GAPDH served as loading controls throughout. Proteins were detected at the expected molecular weights (TrkB.FL: 140 kD, TrkB.t1: 90 kD, HSP-70: 70 kD, PSD-95: 95 kD, syn: 37 kD, Akt: 63 kD; GAPDH: 37 kD). Adolescent mice are P42, adult mice are P90. Means \pm SEMs, * $p < .05$.

Table 1a

Time spent immobile (raw values) for adult and adolescent mice in the forced swim test.

Age	Drug	n	Time spent immobile (\pm SEM)	Statistics
Adult	Saline	6	141.53 \pm 10.5 s	$t_{(11)} = 0.25, p = .807$
Adult	Fasudil	7	137.80 \pm 10.5 s	
Adolescent	Saline	7	157.33 \pm 17.02 s	$t_{(14)} = 2.38, p = .032$
Adolescent	Fasudil	9	101.92 \pm 15.7 s	

Table 1b

Latency to approach food (raw values) for adult and adolescent mice in the novelty suppressed feeding test.

Age	Drug	n	Latency to approach (\pm SEM)	Statistics
Adult	Saline	10	27.08 \pm 4.5 s	$t_{(18)} = 0.74, p = .47$
Adult	Fasudil	10	22.69 \pm 3.9 s	
Adolescent	Saline	8	61.37 \pm 17.4 s	$t_{(14)} = 2.04, p = .06$
Adolescent	Fasudil	8	24.62 \pm 6.6 s	

adult, vs. adolescent, mice. Because drug-naïve adult and adolescent mice differed in their baseline behaviors (Table 1), we normalized fasudil-treated mice to their same-age control counterparts. Fasudil did not decrease time spent immobile in the FST in adult mice, indicating that the antidepressant-like effect is specific to adolescents [$t_{(14)} = 2.57, p = .022$] (Fig. 2a, Table 1a). Even at higher doses, fasudil did not have antidepressant-like effects in adults (Fig. S4a-c). Further, fasudil had no impact on latency to approach food in the NSF test in

adult mice, while decreasing latency in adolescent mice [adult vs. adolescent: $t_{(16)} = 2.52, p = .023$] (Fig. 2b, Table 1b).

We then tested whether fasudil also differentially impacts protein levels of TrkB and Akt, two molecular factors associated with antidepressant-like action, in the vmPFC, considered a locus of antidepressant action. Fasudil increased the proportion of active, full-length TrkB (TrkB.FL) relative to inactive, truncated TrkB (TrkB.t1) in adolescents, but not adults [$t_{(12)} = 4.54, p = .0007$] (Fig. 2c). Thus, the antidepressant-like effects of fasudil may be associated with down-regulation of the TrkB.t1 isoform, up-regulation of the TrkB.FL, or an imbalance of the two. We think it likely that up-regulation of TrkB.FL, and not modification of TrkB.t1, is involved in the antidepressant-like effects of fasudil in the FST for two reasons: Firstly, viral-mediated overexpression of TrkB.t1 in the vmPFC did not block the antidepressant-like efficacy of fasudil in the FST (Fig. S5). Meanwhile, fasudil increased levels of the TrkB.FL signaling partner, Akt, in adolescent mice [$t_{(16)} = 2.67, p = .017$] (Fig. 2d).

To evaluate whether the fasudil-mediated elevation in Akt contributed to its antidepressant-like effects, we identified a systemic dose of the Akt inhibitor, MK-2206, that reduced Akt-mediated signaling (phosphorylation) in the vmPFC [$t_{(9)} = 3.05, p = .014$] (Fig. 2e). We then co-administered it with fasudil prior to the FST. MK-2206 alone increased immobility time, and it blocked any behavioral effect of fasudil [$F_{(2,17)} = 4.32, p = .031$] (Fig. 2f). Thus, enhancing Akt protein levels, and thereby, Akt-mediated signaling, may be one mechanism by which fasudil exerts its therapeutic-like effect.

Finally, fasudil also elevated PSD-95, a postsynaptic marker of excitatory synapses, in adolescents but not in adults

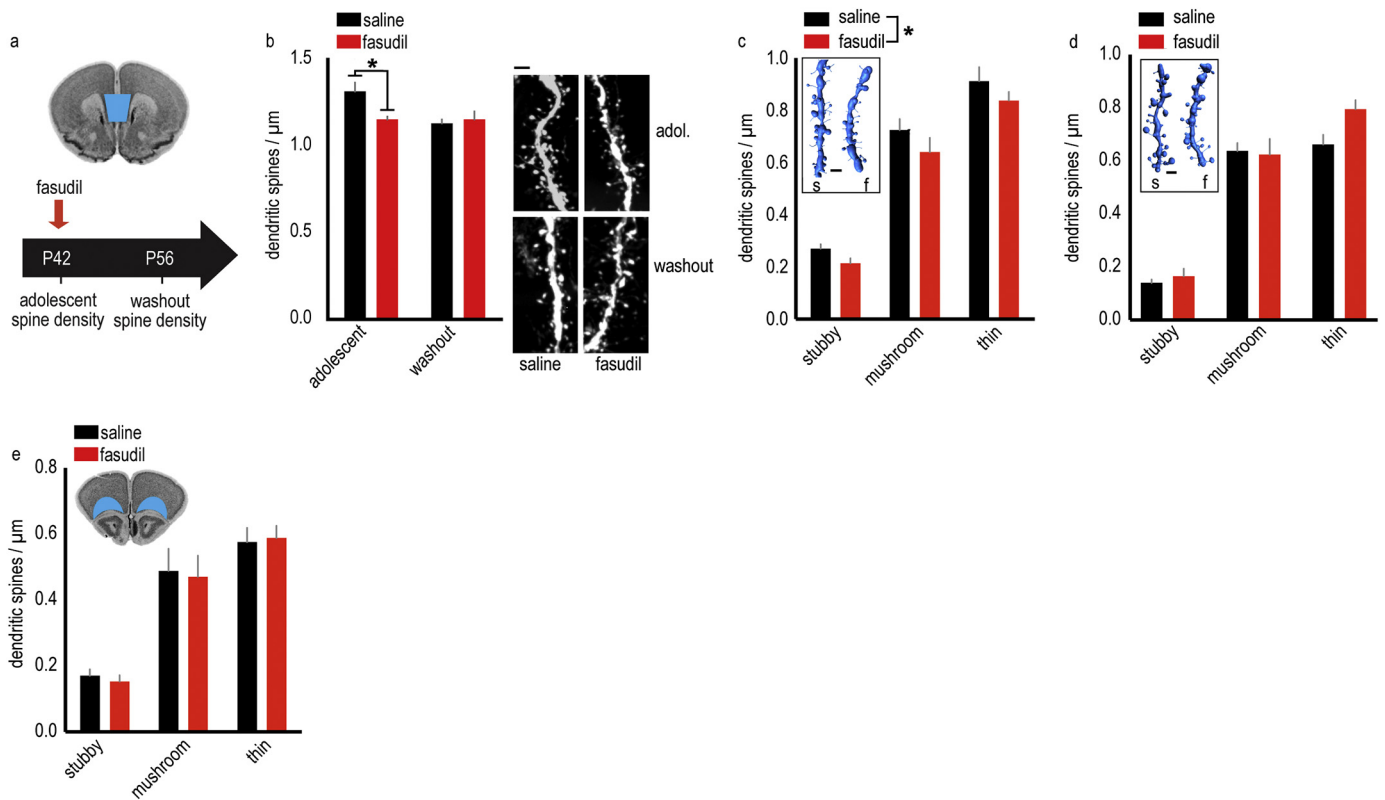


Fig. 3. ROCK inhibition expedites dendritic spine pruning in the adolescent female vmPFC. **A.** Timeline of experimental events: fasudil was administered at P42, and dendritic spines on layer V neurons in the vmPFC (represented in blue on a coronal section from the Mouse Brain Library (Rosen et al., 2000)) were quantified either 1 h following administration (termed “adolescent”) or after a two-week washout period (termed “washout”). **B.** Fasudil reduces dendritic spine density in adolescence, recapitulating adult-like spine densities. In adulthood, mice with a history of fasudil treatment (washout group) have typical dendritic spine densities. Representative dendritic segments are adjacent. $n = 6\text{--}7/\text{group}$. **C.** 3D reconstructions of dendritic spines from the adolescent group reveal a non-specific loss of stubby, mushroom and thin spines. $n = 7/\text{group}$. Inset: Representative dendrite reconstructions. **D.** 3D reconstructions of dendritic spines from the adult mice with a history of fasudil reveal no long-term effects of the drug. $n = 6/\text{group}$. Inset: Representative dendrite reconstructions. **E.** In the adjacent OFC (represented in blue on a coronal section from the Mouse Brain Library (Rosen et al., 2000)), we find no changes in dendritic spine densities. $n = 5\text{--}6/\text{group}$. Means + SEMs, $*p < .05$. Scale bars = 2 μm . (For interpretation of the references to colour in this figure legend, the reader is referred to the web version of this article.)

[$t_{(12)} = 6.10, p < .0001$] (Fig. 2g). Fasudil did not have any effect on synaptophysin, a presynaptic marker, in adolescent or adult mice [$t_{(13)} = 1.03, p = .321$] (Fig. 2h), suggesting that the elevation in PSD-95 is indicative of strengthened synapses, rather than an over-abundance of synapses (Beique and Andrade, 2003; Navone et al., 1986).

2.3. Acute ROCK inhibition expedites vmPFC dendritic spine pruning in adolescence

Adolescence is characterized by considerable structural plasticity in the PFC, culminating in the pruning of dendritic spines and the stabilization of remaining synapses. We used confocal microscopy and Yellow Fluorescent Protein (YFP)-expressing mice to determine whether the same amount of fasudil that had antidepressant-like effects (3 injections of 10 mg/kg over 24 h) also induced structural modifications in the vmPFC. We first quantified dendritic spine densities on layer V excitatory neurons by manually counting dendritic spines 1 h or 2 weeks following fasudil administration at postnatal day (P) 42 (Fig. 3a). Fasudil rapidly eliminated dendritic spines (detectable at 1 h), while the washout groups did not differ [interaction $F_{(1,22)} = 5.75, p = .025$] (Fig. 3b).

Next, an independent rater reconstructed dendrites in 3D, enabling us to classify dendritic spines. This analysis revealed that fasudil reduced the density of all three spine subtypes – stubby, mushroom and thin [main effect of fasudil $F_{(1,36)} = 4.65, p = .038$, no interactions] (Fig. 3c) in the adolescent group, and had no effect on spine subtype in the washout group [main effect $F_{(1,30)} = 2.62, p = .12$] (Fig. 3d).

ROCK2 is highly expressed in both the vmPFC and adjacent orbitofrontal cortex (OFC), but dendritic spines within the OFC are pruned according to a comparatively delayed trajectory (Shapiro et al., 2017). Fasudil administration at P42 did not affect dendritic spines in the OFC [main effect $F_{(1,27)} = 0.043, p = .84$, no interactions] (Fig. 3e). Together, these findings suggest that fasudil expedites age-typical dendritic spine elimination.

2.4. Intact PFC-dependent learning and memory in fasudil-treated mice

Dendritic spine pruning during adolescence is a critical component of typical maturation, however excessive pruning is likely detrimental. Thus, we felt it important to confirm that fasudil did not negatively impact cognitive function and behavioral flexibility in adolescents. We tested whether fasudil impacted reward-related motivation in a progressive ratio test, the expression of conditioned fear following Pavlovian fear conditioning, and instrumental reversal learning, three behaviors that are dependent upon the vmPFC, primarily the prelimbic subregion, or a distributed vmPFC-limbic network (Corcoran and Quirk, 2007; Gourley et al., 2010; Gourley et al., 2012b).

Mice were first trained to nose poke in operant conditioning chambers for food reinforcers (Fig. 4a). After the initial training, drug-naïve mice were split into two groups, termed “to be saline” and “to be fasudil,” matched based on their response rates (Fig. 4b). To evaluate the effects of fasudil on reward-related motivation, a vmPFC-dependent function (Gourley et al., 2012b), mice were administered fasudil and transitioned to a progressive ratio schedule of reinforcement, in which

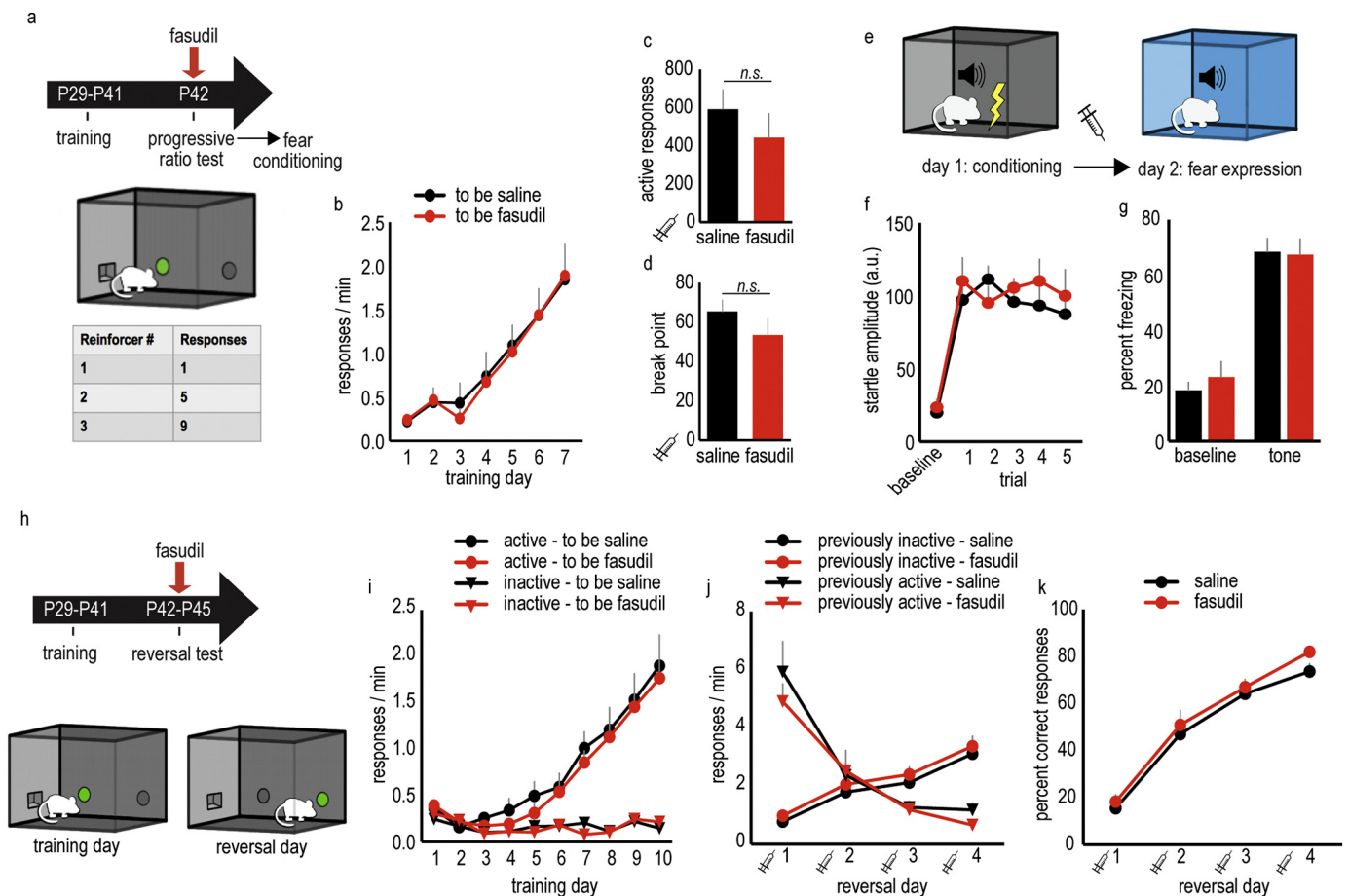


Fig. 4. Repeated, acute ROCK inhibition does not impact performance in PFC-dependent behavioral tasks in adolescent female mice. **A.** Schematic of the progressive ratio task: Mice are initially trained to nose poke for food pellets using a rich reinforcement schedule. Next, the number of responses required to receive a food reinforcer increases by 4, a progressive ratio schedule of reinforcement. **B.** Mice acquired the nose poke responses during training. **C.** Mice received saline or fasudil prior to the progressive ratio test; fasudil did not affect total responses or **(D)** break points. **E.** Schematic of the fear conditioning task: On day 1, a mild shock is paired with a tone. On day 2, mice are exposed to the tone in the absence of the shock in a unique context, a test of tone memory. **F.** Tone-elicited startle increased during training. **G.** Saline or fasudil was delivered prior to the memory expression test on day 2, with no effects detected on either baseline or tone-elicited freezing. **H.** Schematic of the instrumental reversal task: during training, nose poking on one aperture is reinforced by a food pellet, while nose poking on another is not. On test days, the “active” reinforced and “inactive” non-reinforced responses are reversed; thus, mice must modify their response strategies to earn food. **I.** During training, all mice responded preferentially on the active aperture. **J.** Mice received saline or fasudil prior to the reversal days, revealing no effect of fasudil on animals' ability to reverse their response strategies. **K.** Accordingly, response accuracy was also not affected. Throughout, $n = 9\text{--}11/\text{group}$. Syringes indicate timing of drug administration. Means + SEMs. Illustrations courtesy of A. Allen.

the number of responses required for each pellet progressively increases (Fig. 4a). Fasudil did not significantly alter either the number of responses or break points (active responses: [$t_{(16)} = 0.92, p = .37$], break points: [$t_{(16)} = 1.21, p = .25$]; Fig. 4c,d).

Next, the effects of fasudil were evaluated in a fear conditioning test, in which the expression of conditioned fear is dependent upon the vmPFC (prelimbic subregion) (Corcoran and Quirk, 2007) (Fig. 4e). On day 1, a mild foot shock was paired with a tone. Tone-elicited startle progressively increased over 5 trials [$F_{(5,80)} = 15.6, p < .0001$], indicating the mice became conditioned to the tone. We detected no differences in startle amplitude between previously-administered saline mice, and previously-administered fasudil mice [$F_{(1,16)} = 1.49, p = .25$] (Fig. 4f). On day 2, mice were administered saline or fasudil and were placed in distinct chambers, and time spent freezing was calculated before and after the tone to measure the expression of conditioned fear. Fasudil did not affect freezing [$F_{(1,28)} = 0.15, p = .70$] (Fig. 4g).

Lastly, we tested a separate group of mice in an instrumental reversal task. Here, the mice were initially placed in chambers with two nose poke apertures. Responding on one aperture resulted in food pellet delivery, while responding on the other aperture had no effect. After a training period, the “active” and “inactive” apertures were reversed

(Fig. 4h), requiring the mice to modify their response strategies, a process dependent on an extended PFC and hippocampal network (Gourley et al., 2010).

After initial training, drug-naive mice were divided into “to be saline” and “to be fasudil” groups, matched based on their response rates. Mice regardless of group could differentiate between reinforced and non-reinforced responses during training [day \times nose poke interaction $F_{(9,400)} = 21.82, p < .0001$], and we found no group differences in response acquisition [“to be saline” vs. “to be fasudil” $F_{(1,20)} = 0.31, p = .58$, no interactions] (Fig. 4i). In the reversal phase, we identified no interactions between response choice and drug [$F_{(1,19)} = 1.79, p = .20$] or response, drug, and session [$F_{(3,57)} = 0.37, p = .78$], suggesting that fasudil did not impact responding. Consistent with this perspective, fasudil also did not alter overall response rates [no effect of fasudil $F_{(1,19)} = 0.023, p = .882$, no interactions] (Fig. 4j) or response accuracy [no effect of fasudil $F_{(1,19)} = 1.20, p = .287$, no interactions] (Fig. 4k). Importantly, response rates on the newly reinforced aperture increased over time [main effect of day $F_{(3,57)} = 39.75, p < .0001$, no interactions], while the previously reinforced response was inhibited over time [main effect of day $F_{(3,57)} = 44.86, p < .0001$, no interactions] (Fig. 4j). Thus, mice

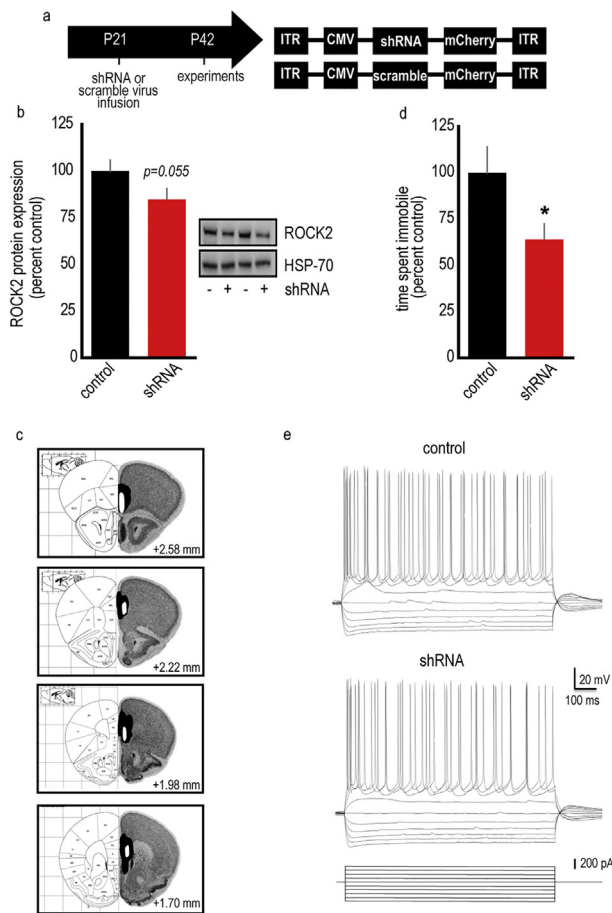


Fig. 5. ROCK2 inhibition selectively in the vmPFC has antidepressant-like effects. **A.** Timeline of experimental events: AAV2s containing an shRNA against ROCK2 or a scrambled sequence as a control and an mCherry tag were infused at P21 in female mice. Experiments were then conducted at P42. **B.** The vmPFC was dissected from fresh frozen brains. Immunoblotting revealed a 17% loss of ROCK2 protein levels. Incomplete loss was expected, given that ROCK2 is expressed in multiple cell types, while our AAV2 would be expected to exhibit neuronal tropism (Watakabe et al., 2015; Zhang et al., 2014). Representative blots are adjacent. HSP-70 served as a loading control. $n = 5-8$ /group. **C.** Separate mice were generated for behavioral testing. Visualization of the mCherry tag confirmed that the viral vector infected the vmPFC. White represents the smallest infusion spread, and black the largest (coronal brain sections with coordinates relative to Bregma from (Paxinos and Franklin, 2002; Rosen et al., 2000)). **D.** shRNA-mediated ROCK2 inhibition has antidepressant-like efficacy in the forced swim test. $n = 10-11$ /group. **E.** We detected no effects of ROCK2 deficiency on baseline physiological properties of layer V vmPFC neurons, suggesting that adolescent ROCK2-deficient neurons were healthy. $n = 9-10$ /group. Representative traces are shown. See table S1 for quantification of physiological parameters. Means + SEMs, $*p < .05$.

could flexibly adjust their behavior and form new reward-related memory, regardless of drug treatment.

2.5. vmPFC-selective ROCK2 silencing has antidepressant-like effects

Our findings indicate that systemic treatment with a ROCK2 inhibitor has antidepressant-like efficacy in adolescent mice, but it was unclear whether these antidepressant-like effects were due to ROCK2 inhibition specifically in the vmPFC. To test this possibility, we generated an shRNA against ROCK2 packaged into an adeno-associated virus (AAV2) (Fig. 5a) and infused it into the vmPFC. Gross tissue punches collected from the vmPFC (containing both infected and non-infected tissue) contained 17% less ROCK2 relative to tissue expressing a scrambled construct [$t_{(11)} = 1.74, p = .055$] (Fig. 5b-c). Site-selective

ROCK2 inhibition decreased immobility in the FST, an antidepressant-like effect [$t_{(19)} = 2.15, p = .045$] (Fig. 5d). Importantly, electrophysiological recordings from shRNA-infected neurons revealed no gross differences in basal membrane properties (Fig. 5e, Table S1), suggesting that ROCK2-deficient neurons retained typical physiological function.

3. Discussion

Adolescent-onset depression is an urgent medical concern due to increased resistance to typical antidepressants and a high risk of recurrence across the lifespan (DeFilippis and Wagner, 2014). Further, few viable treatment options exist. Based on evidence that mammalian PFC neurons undergo considerable structural maturation during adolescence, we investigated the antidepressant-like effects of pharmacological compounds that act on cytoskeletal regulatory, rather than classical neurotransmitter, systems. We find that inhibition of ROCK, a Rho GTPase substrate, has antidepressant-like efficacy in adolescent mice, and that the ROCK inhibitor fasudil is comparable to ketamine and fluoxetine. Fasudil elevates molecular factors associated with antidepressant action and stimulates age-typical dendritic spine elimination in the vmPFC. vmPFC-selective ROCK2 isoform silencing has antidepressant-like behavioral effects, suggesting that fasudil's antidepressant-like actions are due to ROCK2 inhibition in the vmPFC. Despite the vasodilatory properties of ROCK inhibitors, the therapeutic-like dose of fasudil used here does not affect arterial blood pressure (DePoy et al., 2017), highlighting the potential translational appeal of low-dose fasudil for treating adolescent-onset depression.

3.1. ROCK2 inhibition has rapid antidepressant-like effects in adolescent mice

In adolescent mice, fasudil reduced immobility in the FST. This antidepressant-like effect is likely attributable, at least in part, to inhibition of the ROCK2 isoform, given that the highly specific ROCK2 inhibitor SLx-2119 also reduced time spent immobile, even despite modestly blunted locomotor activity. Fasudil was also comparable to ketamine, which has rapid antidepressant onset, and fluoxetine, which is the first-line treatment for adolescent-onset depression. Nevertheless, new treatment approaches are needed: Although fluoxetine is the most effective pharmacotherapy for treating depression in adolescents, approximately half fail to respond (Emslie et al., 1997; Vitiello and Ordonez, 2016). And while ketamine has gained considerable attention as a potential novel antidepressant, it has limited therapeutic potential for adolescents due to safety and abuse concerns, and it may have minimal efficacy in adolescents (Naughton et al., 2014; Nosyreva et al., 2014). To compare the effects of fasudil to the most optimal ketamine response, we used a median split to identify ketamine “responders” and “non-responders.” Our observation that fasudil's antidepressant-like efficacy is comparable to ketamine “responders” highlights the potential of ROCK inhibition as a novel depression treatment option.

One limitation of the FST is that it lacks face validity, meaning, drugs like fluoxetine can affect performance mere minutes after treatment, but require several weeks before affecting clinical populations. The NSF test is sensitive to the therapeutic onset of antidepressants, for instance, requiring chronic administration of typical antidepressants before an effect can be detected (Ramaker and Dulawa, 2017). Thus, it was not surprising that fluoxetine had no effects in the NSF test here. Fasudil-treated mice and ketamine “responders,” however, exhibited decreased latency to approach a novel food, an antidepressant-like effect that suggests that like ketamine (Autry et al., 2011; Li et al., 2010), fasudil may have rapid therapeutic-like potential.

3.2. Fasudil modulates signaling molecules related to antidepressant action

The neurotrophic factor, brain-derived neurotrophic factor (BDNF),

and its high-affinity receptor TrkB are overwhelmingly implicated in the efficacy of chemically distinct antidepressants (Bjorkholm and Monteggia, 2016). The TrkB receptor exists in full-length (TrkB.FL) and truncated (TrkB.t1) isoforms. When activated, TrkB.FL stimulates intracellular signaling cascades to promote neuronal survival and plasticity (Deinhardt and Chao, 2014). TrkB.t1 lacks the intracellular kinase domain, and can serve as dominant negative receptor by binding BDNF and preventing TrkB.FL activation (Deinhardt and Chao, 2014). Fasudil increased the ratio of TrkB.FL/TrkB.t1 in the vmPFC of adolescent but not adult mice here, which would be expected to increase the ability of TrkB.FL to stimulate downstream signaling partners. Our findings are consistent with prior investigations indicating that fasudil increases *Bdnf* *in vitro* (Lau et al., 2012; Yu et al., 2016a; Yu et al., 2016b), given that BDNF stimulates TrkB.FL localization to the cell surface, which then stimulates further TrkB.FL expression (Haapasalo et al., 2002).

Given that fasudil modified TrkB.FL/TrkB.t1 ratios in the vmPFC, the antidepressant-like effects of fasudil may be associated with down-regulation of TrkB.t1, up-regulation of TrkB.FL, or both. We over-expressed *Trkb.t1* in the vmPFC using a viral vector strategy that increases TrkB.t1, but does not impact TrkB.FL or BDNF (immature or mature) (Pitts et al., 2018). *Trkb.t1*-overexpressing mice were sensitive to fasudil in the FST (Fig. S5), suggesting that the antidepressant-like effects of fasudil in this test are not associated with TrkB.t1, *per se*. Nevertheless, our findings do not rule out the possibility that fasudil-mediated TrkB.t1 modification has other consequences. BDNF-TrkB stimulation in the vmPFC restores reward sensitivity in a model of depression (Gourley et al., 2012b). Whether fasudil or other ROCK-regulatory factors have antidepressant-like effects in models of adolescent-onset depression will be tested in future investigations.

Fasudil also increased Akt, a protein downstream of TrkB.FL implicated in antidepressant-like action (Beaulieu, 2012; Li et al., 2010). This pattern is consistent with evidence that ROCK negatively regulates Akt, such that ROCK inhibition stimulates Akt (Ming et al., 2002; Qin et al., 2017; Wolfmum et al., 2004). To test whether fasudil-stimulated Akt was associated with its antidepressant-like effects, we co-administered fasudil with an Akt inhibitor at a dose that reduces Akt phosphorylation in the vmPFC. Akt inhibition occluded the antidepressant-like effects of fasudil in the FST, suggesting that Akt contributes to fasudil's antidepressant-like action.

3.3. ROCK inhibition expedites dendritic spine pruning in the vmPFC during adolescence

Dendritic spines in the PFC are pruned during adolescence (DePoy et al., 2013; Gourley et al., 2012a; Koss et al., 2014; Markham et al., 2013; Milstein et al., 2013; Pattwell et al., 2016; Shapiro et al., 2017) (also, Fig. 3 here). We find that fasudil reduces dendritic spines in the vmPFC, resulting in densities that were 12% lower in fasudil-treated mice than control mice. Although 12% may seem modest, this value exceeds 24-h spine elimination values predicted by *in vivo* imaging of adolescent frontal cortical neurons (Liston and Gan, 2011; Maret et al., 2011; Pattwell et al., 2016; Zuo et al., 2005). Fasudil may have had such potent consequences because administration coincided with the light cycle when mice are typically sleeping, significant because sleep facilitates spine pruning in adolescents (Maret et al., 2011). Importantly, fasudil did not alter responding in 3 behavioral assays dependent on the vmPFC – instrumental responding for food on a progressive ratio schedule, the expression of conditioned freezing following Pavlovian fear conditioning, and instrumental reversal conditioning. Further, dendritic spine densities did not differ between groups following a 2-week washout period, together suggesting that fasudil expedites age-appropriate spine elimination, rather than non-specifically eliminating spines critical to PFC function. Alternatively, fasudil may inhibit new spine formation, stabilizing existing synaptic contacts and resulting in lower spine densities.

Dendritic spine modifications were associated with antidepressant-

like consequences, but it is important to consider the possibility that expediting neurodevelopmental maturation may interfere or conflict with other aspects of adolescent development, for instance, prematurely closing sensitive periods of experience-dependent neuroplasticity.

While fasudil reduced dendritic spine density in the vmPFC, it increased PSD-95, a post-synaptic marker associated with synaptic strength (Beique and Andrade, 2003). Meanwhile, synaptophysin, a presynaptic marker associated with synapse density (Navone et al., 1986), was unaffected. Multiple explanations may account for this pattern. For instance, fasudil might eliminate immature spines (which would presumably not affect synaptic marker expression), while expanding the PSD of existing spines. In our experiments, fasudil did not alter spine head or spine volume, however (not shown), which indirectly argues against this possibility. In mature animals, fasudil can cause dendrite elaboration, rather than pruning (Couch et al., 2010), presumably creating opportunities for dendritic spinogenesis and synaptogenesis. Additional studies using *in vivo* dendrite and dendritic spine imaging may better illuminate the neurobiological functions of ROCK2 across life.

Fasudil-mediated dendritic spine elimination might seem unexpected, given that fasudil and subanesthetic ketamine had common behavioral effects, yet ketamine increases dendritic spine densities in the vmPFC (Li et al., 2010; Phoumthippavong et al., 2016). This discrepancy is likely attributable to our use of adolescent mice, whereas prior ketamine studies generally used adults. As discussed, dendritic spines are pruned at high rates during adolescence, and accordingly, several cytoskeletal regulatory factors are differentially expressed during adolescence vs. adulthood in the PFC (Shapiro et al., 2017). Subanesthetic ketamine has distinct behavioral effects in adolescents vs. adults (Nosyreva et al., 2014; Rocha et al., 2017); how it impacts dendritic spines in adolescents vs. adults remains, to our knowledge, unresolved.

Fasudil did not affect dendritic spines in the OFC. We believe that this outcome is attributable to the relatively delayed maturation of the OFC compared to the vmPFC. In humans, medial PFC white matter volume reaches an adult-like state earlier than in the OFC (Tamnes et al., 2010). In rodents, medial PFC volume peaks at ~P24, while OFC volume peaks later, at ~P30 (Uylings and van Eden, 1990; van Eden and Uylings, 1985). On layer V neurons, dendritic spine densities in the vmPFC drop considerably between P31 to 42, whereas in the OFC, dendritic spine densities decline later, between P39 and P56 (Shapiro et al., 2017). The OFC densities we collected at P42 here are far more in line with those collected at P31 (adolescence) than P56 (adulthood) in prior reports (DePoy et al., 2013; Gourley et al., 2012a; Shapiro et al., 2017), further supporting the notion that dendritic spine pruning in the OFC lags that in the vmPFC. We speculate that ROCK inhibition could facilitate dendritic spine pruning in the OFC at a later, more plastic time point, and/or at a dendritic region not imaged here. Nevertheless, our current findings suggest that dendritic spine plasticity on layer V OFC neurons is not obviously required for the antidepressant-like consequences of fasudil.

3.4. Selective ROCK2 inhibition in the vmPFC has antidepressant-like effects

Our findings build upon previous studies regarding ROCK2 in mature rodents. Certain similarities and differences are worth noting: First, while chronic fasudil administration blocks stress-induced depression-like behaviors and dendritic spine loss on hippocampal CA1 neurons in adult male rats, it notably fails to alter forced swimming in stress-naïve adults (Garcia-Rojo et al., 2017). We similarly find no effect of fasudil in adult stress-naïve mice, despite repeatedly detecting antidepressant-like actions in adolescent mice. In a separate study, the pan-ROCK inhibitor, Y-27632, had antidepressant-like effects in the FST in adult naïve male mice (Inan et al., 2015), but in this report, drugs were locally infused into the vmPFC rather than administered systemically, suggesting that

the vmPFC is a key locus of antidepressant action. Given these and our own findings, we generated an shRNA against the ROCK2 isoform specifically, infusing it into the vmPFC prior to adolescence, anticipating maximal knockdown during adolescence. Site-selective ROCK2 inhibition reduced immobility in the FST, an antidepressant-like effect. Ours is thus the first investigation to reveal that selective inhibition of ROCK2 (as opposed to both ROCK1 and 2 isoforms) in the vmPFC has antidepressant-like consequences. Additionally, our experiments used adolescent female rodents, a translational approach addressing a clear medical need.

All together, we report that fasudil has antidepressant-like potential that exceeds that of an existing pharmacotherapy for adolescent-onset depression (fluoxetine). The therapeutic-like effects of fasudil may be due to expediting structural remodeling in the vmPFC and/or Akt. Fasudil did not apparently interfere with vmPFC function, which was expected, as some studies have suggested that fasudil may even have cognitive enhancing effects (DePoy et al., 2017; Huentelman et al., 2009; Swanson et al., 2017; Zimmermann et al., 2017). Future investigations should evaluate the antidepressant-like utility of ROCK inhibitors in validated preclinical models, as our findings suggest that such strategies may be particularly suitable for adolescents suffering from depression.

4. Methods

Subjects. Subjects were C57BL/6 mice (Jackson Labs). Mice used for dendritic spine analyses expressed *thy1*-derived YFP (H-line from: (Feng et al., 2000)) and were fully back-crossed onto a C57BL/6 background. Due to heightened risk of depression in women (Kuehner, 2017), female mice were used unless otherwise noted.

Mice referred to as “adolescent” were P41–42 (Spear, 2000), and adult mice were ~10–13 weeks old. Mice were maintained on a 12-h light cycle (0700 on) and provided food and water *ad libitum*. Procedures were Emory University IACUC-approved.

4.1. Drugs, timing of injections, and experimental groups

Mice were administered fasudil (LKT Laboratories; 10 mg/kg (Swanson et al., 2017) in the main text and up to 30 mg/kg in the supplementary materials, as indicated graphically). Fasudil was dissolved in Phosphate Buffered Saline (PBS) and delivered *i.p.* Other drugs were: SLx-2119 (Medchem Express; 70 mg/kg *i.p.* in DMSO) (adapted from (Zanin-Zhorov et al., 2014)); fluoxetine (LKT Laboratories; 5 mg/kg *i.p.* in PBS) (Doosti et al., 2013); ketamine (Med-Vet International; 3 mg/kg *i.p.* in PBS) (Franceschelli et al., 2015); or MK-2206 (Medchem Express; 50 mg/kg *i.p.* in 10% DMSO and PBS) (adapted from (Hirai et al., 2010)). Volumes were 1 ml/100 g with the exception of SLx-2119, which was administered in a volume of 0.5 ml/100 g to minimize exposure to the DMSO vehicle.

Unless otherwise noted, ketamine and fluoxetine were administered once, 30 min prior to behavioral testing or euthanasia. MK-2206 was administered 90 min prior to FST. Fasudil and SLx-2119 were administered 23, 5 and 1 h prior to the FST, NSF, progressive ratio test, fear conditioning test or euthanasia. For locomotor monitoring experiments, drugs were administered at the start of testing, then locomotion was monitored for the durations indicated in the figures. In the reversal learning test, mice were injected daily over the course of 4 days, 1 h before each daily test session. This timing of injections allowed for detection of both acute, as well as accumulated, effects of fasudil, if any. Throughout, control mice received the corresponding vehicles at the corresponding times. The varied control groups in a given experiment did not differ and were combined. Separate cohorts of mice were used for the FST, NSF, reversal test, and collection of post-mortem measures. Mice tested in the progressive ratio test were next tested in the fear conditioning test.

4.2. FST

FSTs were conducted by placing mice in a beaker filled to 10 cm with 25 ± 0.5 °C water changed between animals. Six-minute sessions were videotaped under dim light, and time spent immobile in the last 4 min was scored (Porsolt et al., 1977). Immobility was defined as only movements necessary to keep the head above water and was scored by a single blinded rater.

Surgical procedures can interfere with performance in the FST (Fan et al., 2014). Thus, in mice that received intracranial infusions, 2 FSTs were conducted 24 h apart, the first serving to habituate mice to the procedure. Immobility during the second test was recorded and scored and is reported.

4.3. NSF

Mice were food-restricted for approximately 6 h prior to testing and were then individually placed in a large clean cage (18" X 9.5" X 8.5") with a high-fat food pellet placed in the center. Mice were placed in the corner of the cage, and latency to approach the food, defined as nasal or oral contact, was recorded by a single blinded rater.

4.4. Locomotor activity

Mice were placed individually in clean cages positioned in customized locomotor monitoring frames (Med-Associates) equipped with 16 photobeams. Total beam breaks were collected over the duration of the test. The duration of each test is indicated in the figures.

4.5. Progressive ratio task

Adolescent mice were food restricted, given only enough chow to allow for typical weight gain according to Jackson Laboratories growth curves. Between P29–P41, mice were trained to nose poke for food reinforcers (20 mg grain-based Bio-Serv Precision Pellets) in illuminated Med-Associates operant conditioning chambers equipped with two poke recesses and a food magazine. Responding on one recess was reinforced using a fixed ratio 1 schedule, meaning, one pellet was delivered after each nose poke. All mice received 7 days of training, and sessions were 60 min each.

On P42, mice were tested using a progressive ratio schedule of reinforcement in which the response requirement increased by 4 with each pellet delivery (*i.e.*, 1,5,9, $x + 4$). Sessions ended at 180 min or when mice did not respond for 5 min. The dependent variables were the break point ratios, defined as the highest number of responses the mice were willing to complete to receive a pellet, and total responses. Mice were returned to *ad libitum* feeding and allowed ~1 week of recovery before fear conditioning.

4.6. Auditory fear conditioning

SR-LAB Startle Response Systems (San Diego Instruments), equipped with programmable animal shockers, were used. A piezoelectric accelerometer mounted below animal enclosures (5" (L) x 1 1/2" (ID)) rectified, digitized and recorded startle amplitudes on SR-LAB software. Mice were placed in the enclosures, and after 1 min, they received the first of 5 tone + shock pairings. Each trial consisted of a 30-s tone (6 kHz, 88 dB) that ended with a 1 s, 0.6 mA footshock. Tone-elicited startle amplitudes were used to confirm conditioning. The following day, mice were placed in contextually distinct chambers, habituated for 1 min, then presented with 15 30-s tones over 15 min in the absence of shock. The percentage of time freezing during these 30-s trials, and in the 30-s period prior to the first tone, were recorded using a USB video camera, and compared between groups. The absence of any movement excluding respiration was considered freezing and calculated by BORIS software (Friard and Gamba, 2016).

4.7. Instrumental reversal task

Adolescent mice were food restricted, given only enough chow to allow for typical weight gain according to Jackson Laboratories growth curves. Between P29–P41, mice were trained to nose poke for 20 mg grain-based food reinforcers (Bio-Serv Precision Pellets) using standard illuminated Med-Associates conditioning chambers equipped with 2 nose poke apertures located on opposite sides of one wall. Responding was reinforced on 1 of the 2 nose poke apertures according to a variable ratio 2 schedule of reinforcement. Mice were trained once/day for 10 days. Sessions were 25 min long on training days 1–5, and 50 min long on training days 6–10.

Next, from P42–P45, mice were subjected to an instrumental reversal test (Gourley et al., 2010). During the test, responding on the previously inactive aperture was reinforced, whereas the previously-reinforced response no longer generated food. Thus, mice were required to “reverse” their response to continue to obtain food. Response rates and percentages of total responses that were “correct” were compared between groups.

4.8. Immunoblotting

Mice were euthanized by rapid decapitation following brief anesthesia with isoflurane. The timing of euthanasia corresponded with the timing of behavioral tests (i.e., 1 h following the final fasudil injection or 30 min following the ketamine and fluoxetine injections). Brains were extracted and frozen at -80°C and then sectioned using a chilled brain matrix into 1 mm sections. Tissue punches expected to contain the prelimbic and infralimbic PFC regions were extracted using a 1 mm diameter tissue core, and were homogenized by sonication in lysis buffer (200 μl : 137 mM NaCl, 20 mM tris-HCl (pH = 8), 1% igeal, 10% glycerol, 1:100 Phosphatase Inhibitor Cocktails 2 and 3 (Sigma), 1:1000 Protease Inhibitor Cocktail (Sigma)) and stored at -80°C . Protein concentrations were determined using a Bradford colorimetric assay kit (Pierce).

Equal amounts of protein were separated by SDS-PAGE on either 4–20% or 7.5% gradient tris-glycine gels (Bio-rad). Following transfer to PVDF membrane, blots were blocked with 5% nonfat milk for 1 h, incubated first with primary antibodies at 4°C overnight and then with horseradish peroxidase secondary antibodies (anti-mouse, 1:10,000, Jackson ImmunoResearch, anti-rabbit, 1:10,000, Vector Labs) for 1 h. Immunoreactivity was assessed using a chemiluminescence substrate (Pierce) and measured using a ChemiDoc MP Imaging System (Bio-rad). Densitometry values were normalized to the corresponding loading control. All densitometry values were then normalized to the control sample mean from the same membrane in order to control for variance in fluorescence between gels. All immunoblots were replicated at least twice.

4.9. Primary antibodies

See Table 2.

Table 2
Antibodies used in this study.

Antibody	Host	Manufacturer, product number, lot number	Conc.
anti-HSP70	Mouse-monoclonal	Santa Cruz Biotechnology #7298, lot F0413	1:5000
anti-ROCK2	Rabbit-polyclonal	Abcam #71598, lot Gr51275-1	1:1000
anti-PSD95	Rabbit-monoclonal	Cell Signaling #3450, lot 2	1:1000
anti-synaptophysin	Rabbit-monoclonal	Abcam #32127, lot Gr196393-2	1:20,000
anti-TrkB	Rabbit-monoclonal	Cell Signaling #4603, lot 3	1:250
anti-AKT	Rabbit-monoclonal	Cell Signaling #4691, lot 17	1:1000
anti-phospho AKT (Thr308)	Rabbit-monoclonal	Cell Signaling #2865, lot 13	1:500
anti-GAPDH	Mouse-monoclonal	Sigma #G8795, lot 044m4808v	1:5000

4.10. Dendritic spine analyses

Transgenic mice expressing YFP in layer V cortical pyramidal neurons were treated with fasudil or saline 23, 5 and 1 h before euthanasia by rapid decapitation at P42, the same timing and age used for behavioral studies. Another group was treated identically, and then euthanized 2 weeks following treatment (termed “washout” in the corresponding figure). Brains were submerged in chilled 4% paraformaldehyde for 48 h, then transferred to 30% w/v sucrose solution for 72 h and sectioned into 50 μm thick coronal sections on a microtome held at -15°C .

Neurons in the vmPFC and adjacent OFC were imaged using a Leica SP8 confocal laser scanning microscope. Z-steps were collected with a 100×1.4 numerical aperture objective using a 0.1 μm step size. We confirmed at $10 \times$ magnification that the images were collected from the vmPFC, corresponding to Figs. 14–16, and from the OFC, corresponding to Figs. 7–13, of *The Mouse Brain in Stereotaxic Coordinates* (Paxinos and Franklin, 2002). Dendrites were 15–25 μm in length and located 25–150 μm from the cell body, were clearly discernible and not interrupted by other dendrites in the field of view that could obstruct our ability to quantify spines. 4–10 dendrites were imaged per mouse, with each mouse considered an independent sample.

Dendritic spines were first manually counted by a blinded rater. Next, dendritic spines were reconstructed in 3 dimensions using Imapris software (Bitplane), as described (Swanson et al., 2017). Briefly, a dendrite segment 15–25 μm in length was traced using the autodepht function. Dendritic spine heads were manually identified, and Imapris FilamentTracer processing algorithms were used to calculate morphological parameters. Dendritic spines were then classified as stubby, mushroom and thin. Stubby spines were defined as those with a length $< 0.6 \mu\text{m}$, and a head to neck ratio of ≤ 1.5 . Mushroom spines had a head to neck ratio of > 1.5 . Thin spines were defined as spines with a length $\geq 0.6 \mu\text{m}$, and a head to neck ratio of ≤ 1.5 . Dendritic spines that had a head to neck ratio of > 1.5 , but had a head size of $\leq 0.4 \mu\text{m}$, were also classified as thin. All spines had a length $< 4.0 \mu\text{m}$ (Bourne and Harris, 2007; Radley et al., 2013; Swanger et al., 2011).

4.11. ROCK2 shRNA and stereotaxic surgery

shRNA against ROCK2 and a scrambled control construct were generated by the Emory Cloning Core. The following sequences were used: shRNA 5-CAATGAAGCTTCTTAGTAA and scrambled: 5-GGACTA CTCTAGACGTATA (Herskowitz et al., 2013). The constructs were packaged into an AAV2 with a CMV promoter and an mCherry tag by the Emory Viral Vector Core. Titers were 5.3×10^{10} vg/ml and 1.5×10^{11} vg/ml for the shRNA and scrambled viruses, respectively.

Intracranial surgery was performed at P21. Mice were anesthetized with ketamine and dexdormitor. Stereotaxic coordinates were located on the leveled skull, and viruses were infused in a volume of 0.5 μl at AP + 2.0, DV-2.8, ML ± 0.1 (Gourley et al., 2012b) over 5 min with needles left in place for an additional 5 min. Mice were then sutured and revived with antisedan (1 mg/kg, i.p.). Mice were allowed to recover for 21 days to allow for viral-mediated ROCK2 silencing (Ahmed

et al., 2004; Newman et al., 2015).

4.12. Histology

After testing, mice were killed by rapid decapitation following brief anesthesia with isoflurane, and brains were extracted and submerged in chilled 4% paraformaldehyde for 48 h, then transferred to chilled 30% w/v sucrose for histological processing. Infusion sites from the shRNA experiment were verified through visualization of the mCherry tag. Brains were sectioned into 50 μm -thick sections on a microtome held at $-15\text{ }^{\circ}\text{C}$. Sections were mounted, coverslipped and imaged.

4.13. Electrophysiology

Electrophysiological experiments were conducted between P41–P44, following infusions of ROCK2 shRNA-expressing viral vectors as described above. Mice were anesthetized with isoflurane and brains were rapidly dissected and immersed in a $4\text{ }^{\circ}\text{C}$ 95–5% oxygen/carbon dioxide oxygenated cutting solution (in mM: NaCl (130), NaHCO₃ (30), KCl (3.5), KH₂PO₄ (1.1), MgCl₂ (6.0), CaCl₂ (1.0), glucose (10), and supplemented with kynurenic acid (2.0)). 350 μm sections containing the vmPFC were collected and submerged for 1 h in $32\text{ }^{\circ}\text{C}$ oxygenated artificial cerebrospinal fluid made up of: NaCl (130), NaHCO₃ (30), KCl (3.5), KH₂PO₄ (1.1), MgCl₂ (1.3), CaCl₂ (2.5), and glucose (10). Slices were then mounted to a recording chamber on the fixed stage of a Leica DM6000 FS microscope and continuously perfused with oxygenated $32\text{ }^{\circ}\text{C}$ artificial cerebrospinal fluid at a speed of $\sim 2\text{ ml/min}$. A potassium-based patch solution was made RNase-free and supplemented with an RNase inhibitor (1 U/ μl ; Life Technologies). Whole-cell recordings and analyses from mCherry and YFP co-expressing cells were then obtained as previously described (Andero et al., 2016).

4.14. Statistical analyses

t-tests and one- or two-factor ANOVAs were performed using SigmaStat and Graphpad Prism, with $\alpha \leq 0.05$ to detect differences in immobility scores, normalized densitometry values, latencies to approach food, and dendritic spine densities. Response rates and locomotor counts from the instrumental conditioning and locomotor assays were compared by repeated measures ANOVAs. Tukey's post-hoc comparisons were used in the case of significant interactions or main effects between > 2 groups. Comparisons were two-tailed except to compare immobility scores between control and SLX-2119-treated mice and ROCK2 expression in tissues subjected to ROCK2 shRNA infusion, in which case, *a priori* hypotheses warranted one-tailed approaches. Throughout, values lying two standard deviations outside the mean were considered outliers and excluded. Individual group sizes and number of outliers excluded from each experimental group are compiled in Tables S2 and S3 respectively.

Role of authors

Authors had access to the data in the study and take responsibility for the integrity of the data and accuracy of the data analyses. Study concept and design: LS and SG. Acquisition of data: LS, HK and JG. Analysis and interpretation of data: LS, HK, JG and SG. Manuscript composition: LS. Critical revision of the manuscript for important intellectual content: LS and SG. Statistical analyses: LS and SG. Obtained funding: LS, DR and SG. Administrative, technical, and material support: DR and SG. Study supervision: SG.

Conflict of interest

None of the authors has any conflicts to disclose.

Acknowledgements

We thank Dr. Alonzo Whyte and Weibo Fu for their assistance in imaging and reconstructing dendritic spines. We thank A. Allen for assistance with the experiments and illustrations in Fig. 4, Elizabeth Hinton for her assistance with forced swim testing and Apoorva Gangavelli for her assistance with operant conditioning. The work in the SLG lab was supported by NIH (National Institutes of Health) 5T32GM008602-17, F31MH109208, R01MH101477 and R01MH117103. The work in the DGR lab was supported by NIHMH072908. The Yerkes National Primate Research Center was supported by the Office of Research Infrastructure Programs/OD P51OD011132. This research project was also supported in part by the Viral Vector Core of the Emory Neuroscience NINDS Core Facilities grant, P30NS055077, and by the Emory Integrated Genomics Core (EIGC), which is subsidized by the Emory University School of Medicine and is one of the Emory Integrated Core Facilities. Additional support was provided by the Georgia Clinical & Translational Science Alliance of the NIH under Award Number UL1TR002378. The content is solely the responsibility of the authors and does not necessarily reflect the official views of the NIH.

Appendix A. Supplementary data

Supplementary data to this article can be found online at <https://doi.org/10.1016/j.nbd.2018.12.015>.

References

- Ahmed, B.Y., et al., 2004. Efficient delivery of Cre-recombinase to neurons in vivo and stable transduction of neurons using adeno-associated and lentiviral vectors. *BMC Neurosci.* 5, 4.
- Andero, R., et al., 2016. Amygdala-dependent molecular mechanisms of the Tac2 pathway in fear learning. *Neuropsychopharmacology* 41, 2714–2722.
- Autry, A.E., et al., 2011. NMDA receptor blockade at rest triggers rapid behavioural antidepressant responses. *Nature* 475, 91–95.
- Beaulieu, J.M., 2012. A role for Akt and glycogen synthase kinase-3 as integrators of dopamine and serotonin neurotransmission in mental health. *J. Psychiatry Neurosci.* 37, 7–16.
- Beique, J.C., Andrade, R., 2003. PSD-95 regulates synaptic transmission and plasticity in rat cerebral cortex. *J. Physiol.* 546, 859–867.
- Bjorkholm, C., Monteggia, L.M., 2016. BDNF - a key transducer of antidepressant effects. *Neuropharmacology* 102, 72–79.
- Bourgeois, J.P., et al., 1994. Synaptogenesis in the prefrontal cortex of rhesus monkeys. *Cereb. Cortex* 4, 78–96.
- Bourne, J., Harris, K.M., 2007. Do thin spines learn to be mushroom spines that remember? *Curr. Opin. Neurobiol.* 17, 381–386.
- Chen, M., et al., 2013. Fasudil and its analogs: a new powerful weapon in the long war against central nervous system disorders? *Expert Opin. Investig. Drugs* 22, 537–550.
- Corcoran, K.A., Quirk, G.J., 2007. Activity in prefrontal cortex is necessary for the expression of learned, but not innate, fears. *J. Neurosci.* 27, 840–844.
- Couch, B.A., et al., 2010. Increased dendrite branching in AbetaPP/PS1 mice and elongation of dendrite arbors by fasudil administration. *J. Alzheimers Dis.* 20, 1003–1008.
- DeFilippis, M., Wagner, K.D., 2014. Management of treatment-resistant depression in children and adolescents. *Paediatr. Drugs* 16, 353–361.
- Deinhardt, K., Chao, M.V., 2014. Trk receptors. *Handb. Exp. Pharmacol.* 220, 103–119.
- DePoy, L.M., et al., 2013. Developmentally divergent effects of Rho-kinase inhibition on cocaine- and BDNF-induced behavioral plasticity. *Behav. Brain Res.* 243, 171–175.
- DePoy, L.M., et al., 2017. Induction and blockade of adolescent cocaine-induced habits. *Biol. Psychiatry* 81, 595–605.
- Doosti, M.H., et al., 2013. Impacts of early intervention with fluoxetine following early neonatal immune activation on depression-like behaviors and body weight in mice. *Prog. Neuro-Psychopharmacol. Biol. Psychiatry* 43, 55–65.
- dos Remedios, C.G., et al., 2003. Actin binding proteins: regulation of cytoskeletal microfilaments. *Physiol. Rev.* 83, 433–473.
- Duffy, P., et al., 2009. Rho-associated kinase II (ROCKII) limits axonal growth after trauma within the adult mouse spinal cord. *J. Neurosci.* 29, 15266–15276.
- Emslie, G.J., et al., 1997. A double-blind, randomized, placebo-controlled trial of fluoxetine in children and adolescents with depression. *Arch. Gen. Psychiatry* 54, 1031–1037.
- Fan, D., et al., 2014. Enriched environment attenuates surgery-induced impairment of learning, memory, and neurogenesis possibly by preserving BDNF expression. *Mol. Neurobiol.* 53, 344–354.
- Feng, G., et al., 2000. Imaging neuronal subsets in transgenic mice expressing multiple spectral variants of GFP. *Neuron* 28, 41–51.
- Franceschelli, A., et al., 2015. Sex differences in the rapid and the sustained

- antidepressant-like effects of ketamine in stress-naïve and “depressed” mice exposed to chronic mild stress. *Neuroscience* 290, 49–60.
- Friard, O., Gamba, M., 2016. BORIS: a free, versatile open-source evening-logging software for video/audio coding and live observations. *Methods Ecol. Evol.* 7, 1325–1330.
- Garcia-Rojo, G., et al., 2017. The ROCK inhibitor fasudil prevents chronic restraint stress-induced depressive-like behaviors and dendritic spine loss in rat hippocampus. *Int. J. Neuropsychopharmacol.* 20, 336–345.
- Gourley, S.L., et al., 2010. Dissociable regulation of instrumental action within mouse prefrontal cortex. *Eur. J. Neurosci.* 32, 1726–1734.
- Gourley, S.L., et al., 2012a. Arg kinase regulates prefrontal dendritic spine refinement and cocaine-induced plasticity. *J. Neurosci.* 32, 2314–2323.
- Gourley, S.L., et al., 2012b. Action control is mediated by prefrontal BDNF and glucocorticoid receptor binding. *Proc. Natl. Acad. Sci. U. S. A.* 109, 20714–20719.
- Greenberg, P.E., et al., 2015. The economic burden of adults with major depressive disorder in the United States (2005 and 2010). *J. Clin. Psychiatr.* 76, 155–162.
- Haapasalo, A., et al., 2002. Regulation of TRKB surface expression by brain-derived neurotrophic factor and truncated TRKB isoforms. *J. Biol. Chem.* 277, 43160–43167.
- Harbom, L.J., et al., 2018. The effect of rho kinase inhibition on morphological and electrophysiological maturity in iPSC-derived neurons. *Cell Tissue Res.*
- Herskowitz, J.H., et al., 2013. Pharmacologic inhibition of ROCK2 suppresses amyloid-beta production in an Alzheimer's disease mouse model. *J. Neurosci.* 33, 19086–19098.
- Hirai, H., et al., 2010. MK-2206, an allosteric Akt inhibitor, enhances antitumor efficacy by standard chemotherapeutic agents or molecular targeted drugs in vitro and in vivo. *Mol. Cancer Ther.* 9, 1956–1967.
- Huentelman, M.J., et al., 2009. Peripheral delivery of a ROCK inhibitor improves learning and working memory. *Behav. Neurosci.* 123, 218–223.
- Huttenlocher, P.R., Dabholkar, A.S., 1997. Regional differences in synaptogenesis in human cerebral cortex. *J. Comp. Neurol.* 387, 167–178.
- Inan, S.Y., et al., 2015. Infralimbic cortex Rho-kinase inhibition causes antidepressant-like activity in rats. *Prog. Neuro-Psychopharmacol. Biol. Psychiatry* 57, 36–43.
- Isacson, G., Rich, C.L., 2014. Antidepressant drugs and the risk of suicide in children and adolescents. *Paediatr. Drugs.* 16, 115–122.
- Julian, L., Olson, M.F., 2014. Rho-associated coiled-coil containing kinases (ROCK): structure, regulation, and functions. *Small GTPases* 5, e29846.
- Keshavan, M.S., et al., 2014. Changes in the adolescent brain and the pathophysiology of psychotic disorders. *Lancet Psychiatry* 1, 549–558.
- Koleske, A.J., 2013. Molecular mechanisms of dendrite stability. *Nat. Rev. Neurosci.* 14, 536–550.
- Koss, W.A., et al., 2014. Dendritic remodeling in the adolescent medial prefrontal cortex and the basolateral amygdala of male and female rats. *Synapse* 68, 61–72.
- Kuehner, C., 2017. Why is depression more common among women than among men? *Lancet Psychiatry* 4, 146–158.
- Lau, C.L., et al., 2012. Transcriptomic profiling of astrocytes treated with the Rho kinase inhibitor fasudil reveals cytoskeletal and pro-survival responses. *J. Cell. Physiol.* 227, 1199–1211.
- Li, N., et al., 2010. mTOR-dependent synapse formation underlies the rapid antidepressant effects of NMDA antagonists. *Science* 329, 959–964.
- Liston, C., Gan, W.B., 2011. Glucocorticoids are critical regulators of dendritic spine development and plasticity in vivo. *Proc. Natl. Acad. Sci. U. S. A.* 108, 16074–16079.
- Maekawa, M., et al., 1999. Signaling from Rho to the actin cytoskeleton through protein kinases ROCK and LIM-kinase. *Science* 285, 895–898.
- Maret, S., et al., 2011. Sleep and waking modulate spine turnover in the adolescent mouse cortex. *Nat. Neurosci.* 14, 1418–1420.
- Markham, J.A., et al., 2013. Periadolescent maturation of the prefrontal cortex is sex-specific and is disrupted by prenatal stress. *J. Comp. Neurol.* 521, 1828–1843.
- Milstein, J.A., et al., 2013. Olanzapine treatment of adolescent rats causes enduring specific memory impairments and alters cortical development and function. *PLoS One* 8, e57308.
- Ming, X.F., et al., 2002. Rho GTPase/Rho kinase negatively regulates endothelial nitric oxide synthase phosphorylation through the inhibition of protein kinase B/Akt in human endothelial cells. *Mol. Cell. Biol.* 22, 8467–8477.
- Murakoshi, H., et al., 2011. Local, persistent activation of Rho GTPases during plasticity of single dendritic spines. *Nature* 472, 100–104.
- Nakagawa, O., et al., 1996. ROCK-I and ROCK-II, two isoforms of Rho-associated coiled-coil forming protein serine/threonine kinase in mice. *FEBS Lett.* 392, 189–193.
- Naughton, M., et al., 2014. A review of ketamine in affective disorders: current evidence of clinical efficacy, limitations of use and pre-clinical evidence on proposed mechanisms of action. *J. Affect. Disord.* 156, 24–35.
- Navone, F., et al., 1986. Protein p38: an integral membrane protein specific for small vesicles of neurons and neuroendocrine cells. *J. Cell Biol.* 103, 2511–2527.
- Newman, J.P., et al., 2015. Optogenetic feedback control of neural activity. *elife* 4, e07192.
- Nosyreva, E., et al., 2014. Age dependence of the rapid antidepressant and synaptic effects of acute NMDA receptor blockade. *Front. Mol. Neurosci.* 7, 94.
- Pattwell, S.S., et al., 2016. Dynamic changes in neural circuitry during adolescence are associated with persistent attenuation of fear memories. *Nat. Commun.* 7, 11475.
- Paxinos, G., Franklin, K., 2002. *The mouse brain in stereotaxic coordinates*. Gulf Professional Publishing.
- Phoumthippavong, V., et al., 2016. Longitudinal effects of ketamine on dendritic architecture in vivo in the mouse medial frontal cortex. *eNeuro* 3.
- Pitts, E.G., et al., 2018. Bidirectional coordination of actions and habits by TrkB in mice. *Sci. Rep.* 8, 4495.
- Pontrello, C.G., Ethell, I.M., 2009. Accelerators, brakes, and gears of actin dynamics in dendritic spines. *Open Neurosci. J.* 3, 67–86.
- Porsolt, R.D., et al., 1977. Depression: a new animal model sensitive to antidepressant treatments. *Nature* 266, 730–732.
- Qin, T., et al., 2017. Umbelliferone reverses depression-like behavior in chronic unpredictable mild stress-induced rats by attenuating neuronal apoptosis via regulating ROCK/Akt pathway. *Behav. Brain Res.* 317, 147–156.
- Radley, J.J., et al., 2013. Chronic stress-induced alterations of dendritic spine subtypes predict functional decrements in an hypothalamo-pituitary-adrenal-inhibitory prefrontal circuit. *J. Neurosci.* 33, 14379–14391.
- Rakic, P., et al., 1994. Synaptic development of the cerebral cortex: implications for learning, memory, and mental illness. *Prog. Brain Res.* 102, 227–243.
- Ramaker, M.J., Dulawa, S.C., 2017. Identifying fast-onset antidepressants using rodent models. *Mol. Psychiatry* 22, 656–665.
- Rocha, A., et al., 2017. Differences between adolescents and adults in the acute effects of PCP and ketamine and in sensitization following intermittent administration. *Pharmacol. Biochem. Behav.* 157, 24–34.
- Rosen, G., et al., 2000. *The Mouse Brain Library @ www.mbl.org*. *Int. Mouse Genome Conf.* 14, pp. 166.
- Schubert, V., et al., 2006. Localized recruitment and activation of RhoA underlies dendritic spine morphology in a glutamate receptor-dependent manner. *J. Cell Biol.* 172, 453–467.
- Shapiro, L.P., et al., 2017. Differential expression of cytoskeletal regulatory factors in the adolescent prefrontal cortex: Implications for cortical development. *J. Neurosci. Res.* 95, 1123–1143.
- Spear, L.P., 2000. The adolescent brain and age-related behavioral manifestations. *Neurosci. Biobehav. Rev.* 24, 417–463.
- Substance Abuse and Mental Health Services Administration, 2017. *Key Substance Use and Mental Health Indicators in the United States: Results from the 2016 National Survey on Drug Use and Health (HHS Publication No. SMA 17–5044, NSDUH Series H-52)*. Center for Behavioral Health Statistics and Quality, Rockville, MD.
- Swanger, S.A., et al., 2011. Automated 4D analysis of dendritic spine morphology: applications to stimulus-induced spine remodeling and pharmacological rescue in a disease model. *Mol. Brain.* 4, 38.
- Swanson, A.M., et al., 2017. Inhibiting Rho kinase promotes goal-directed decision making and blocks habitual responding for cocaine. *Nat. Commun.* 8, 1861.
- Tamnes, C.K., et al., 2010. Brain maturation in adolescence and young adulthood: regional age-related changes in cortical thickness and white matter volume and microstructure. *Cereb. Cortex* 20, 534–548.
- Uylings, H.B., van Eden, C.G., 1990. Qualitative and quantitative comparison of the prefrontal cortex in rat and in primates, including humans. *Prog. Brain Res.* 85, 31–62.
- van Eden, C.G., Uylings, H.B., 1985. Postnatal volumetric development of the prefrontal cortex in the rat. *J. Comp. Neurol.* 241, 268–274.
- Vitiello, B., Ordonez, A.E., 2016. Pharmacological treatment of children and adolescents with depression. *Expert. Opin. Pharmacother.* 17, 2273–2279.
- Watakabe, A., et al., 2015. Comparative analyses of adeno-associated viral vector serotypes 1, 2, 5, 8 and 9 in marmoset, mouse and macaque cerebral cortex. *Neurosci. Res.* 93, 144–157.
- Wolfrum, S., et al., 2004. Inhibition of Rho-kinase leads to rapid activation of phosphatidylinositol 3-kinase/protein kinase Akt and cardiovascular protection. *Arterioscler. Thromb. Vasc. Biol.* 24, 1842–1847.
- Yu, J.W., et al., 2016a. Synergistic and superimposed effect of bone marrow-derived mesenchymal stem cells combined with fasudil in experimental autoimmune encephalomyelitis. *J. Mol. Neurosci.* 60, 486–497.
- Yu, J.Z., et al., 2016b. Changes of synapses in experimental autoimmune encephalomyelitis by using Fasudil. *Wound Repair Regen.* 24, 317–327.
- Zanin-Zhorov, A., et al., 2014. Selective oral ROCK2 inhibitor down-regulates IL-21 and IL-17 secretion in human T cells via STAT3-dependent mechanism. *Proc. Natl. Acad. Sci. U. S. A.* 111, 16814–16819.
- Zhang, Y., et al., 2014. An RNA-sequencing transcriptome and splicing database of glia, neurons, and vascular cells of the cerebral cortex. *J. Neurosci.* 34, 11929–11947.
- Zhou, Z., et al., 2009. A critical role of Rho-kinase ROCK2 in the regulation of spine and synaptic function. *Neuropharmacology* 56, 81–89.
- Zimmermann, K.S., et al., 2017. Connections of the mouse orbitofrontal cortex and regulation of goal-directed action selection by brain-derived neurotrophic factor. *Biol. Psychiatry* 81, 366–377.
- Zuo, Y., et al., 2005. Development of long-term dendritic spine stability in diverse regions of cerebral cortex. *Neuron* 46, 181–189.